Environ Earth Sci (2010) 61:525–538
DOI 10.1007/s12665-009-0363-3

ORIGINAL ARTICLE

Hydrogeochemistry of Roccamonfina volcano (Southern Italy)

Emilio Cuoco · Giuseppe Verrengia · Stefano De Francesco · Dario Tedesco

Received: 22 April 2009 / Accepted: 4 November 2009 / Published online: 15 December 2009

Abstract This is the first hydro-geochemical investigation carried out on the Roccamonfina Volcanic Complex groundwaters. The chemistry of Roccamonfina waters is defined by water–rock and water–rock–gas interactions. In fact, interactions between rocks of the first eruptive high-K formations and circulating groundwaters are recognized by high K concentrations. On the other hand, inverse concentration of calcium versus alkali metals is related to two different rock interactions occurring in different areas of the volcano: (a) within the caldera where groundwaters flow within latite and pyroclastic formations releasing calcium, and (b) similarly at the base of the volcano where groundwaters flowing from surrounding carbonates got strongly enriched in Ca. These geochemical processes are also associated with K (SE of caldera) and Mg/Ca (in sites located at the NE base of the volcano) decrease. Completely different dynamics occurs at Riardo groundwaters (SE). Here waters are the result of a mix between the Roccamonfina deep aquifer and the carbonate aquifer of the Riardo plain. Rich-CO_2 emissions make these waters strongly mineralized. Minor elements show a similar geochemical behavior of major ions and are crucial defining interactions processes. The evolution of Roccamonfina groundwaters is also evident along the simultaneous enrichment of Ba, Sr, and Ca. Ba increase is the result of deep local carbonate alteration enhanced by CO_2 emissions and, the lower Sr/Ca ratio, from 10 to 2 (ppb/ppm), is also due to the same process. In the light of our results the Roccamonfina aquifer can be schematically divided into two main reservoirs: (a) a superficial aquifer which basically follows the volcanic structure morphology and tectonics and (b) a deeper reservoir, originating within the oldest Roccamonfina volcano ultra potassic lavas and then flowing into the carbonate aquifers of the neighboring plain. Eventually, the chemistry of the Roccamonfina aquifer does not show any specific and visible pollution, contrary to what happens in the volcano surrounding plains. In fact, only 14% of the samples we collected (206) show a NO_3 content >30 mg/l. These sites are all located at the base of the volcano, near the plain.

Keywords Hydrology · Geochemistry · Volcanic groundwaters · Roccamonfina · CO_2 groundwater interactions

Introduction

The Roccamonfina Volcanic Complex (RVC) lies north of Mount Massico within the Garigliano depression, in the north-western part of Campania Region. The magmatism of this area occurred between 550,000 and 150,000 years ago (Rouchon et al. 2008). Three eruptive periods have been recognized: (1) the tephrite-phonolite stratovolcanoes, namely "High-K series", (2) the explosive eruptions of the Brown Leucitic Tuff (BLT) and the White Trachytic Tuff, and finally, (3) the small explosive eruptions forming two lava domes (Latite) inside the caldera close to the eruptive activity.

Electronic supplementary material The online version of this article (doi:10.1007/s12665-009-0363-3) contains supplementary material, which is available to authorized users.

E. Cuoco (✉) · G. Verrengia · S. De Francesco · D. Tedesco
Department of Environmental Sciences,
Second University of Napoli, Caserta, Italy
e-mail: emilio.cuoco@unina2.it

D. Tedesco
Istituto di Geologia Ambientale e Geo-Ingegneria,
CNR, Piazzale Aldo Moro, Rome, Italy

The RVC shows composite geological setting (Rouchon et al. 2008). The different geological features (volcanic products belonging to different periods) are reflected into the high chemical variability of local groundwaters. In this area are present several natural springs showing different chemical features. Mineralized waters are located at the feet of the volcanic edifice, in two main areas: (1) Suio and (2) Riardo. On the other hand, cold water springs are located nearby the Roccamonfina town and close the SE rim of the caldera (Fig. 1).

The present work tries to give through a collection of more than 200 water samples homogeneously distributed on the studied area, an exhaustive description of the several hydrogeochemical processes affecting the Roccamonfina aquifer system and to highlight correlations among chemical parameters and water–rock interaction, local tectonics, and hydrothermal activity in both superficial and deep systems.

Geological setting

The RVC located within the Ernici-Roccamonfina volcanic provenance lies north of Mt. Massico within the Garigliano depression in the north-western Campania region (west-central Italy, Fig. 1) (Peccerillo 2005). The tectonic setting of the northern Campania plays a key role in the RVC emplacement and its morphological evolution (De Rita and Giordano 1996). The tectonic framework and geological map of Roccamonfina volcano are shown in Fig. 1. The Garigliano and Campanian Plain Grabens result from crustal extension during the main rifting of the Tyrrhenian basin. The RVC is contained within the most topographically depressed area of the Garigliano Graben at the intersection of the NW-trending tectonic depression of the Riardo plain. The tectonic evolution of the RVC was controlled by the extensional NW faults of Mount Massico through the Pleistocene (Nicotera and Civita 1969; Ippolito et al. 1973).

The magmatic activity in the RVC occurred between 550,000 and 150,000 years BP (Rouchon et al. 2008). While the timing of the eruptive stages that created the RVC is still a matter of debate (Capuano et al. 1992; Chiesa et al. 1995; De Rita and Giordano 1996; Giannetti 2001; Rouchon et al. 2008), the published works give a clear geological description. The bedrock of the volcano complex consists of Pliocene-lower Pleistocene and Miocenic sandstone and clay sedimentary formations emplaced on

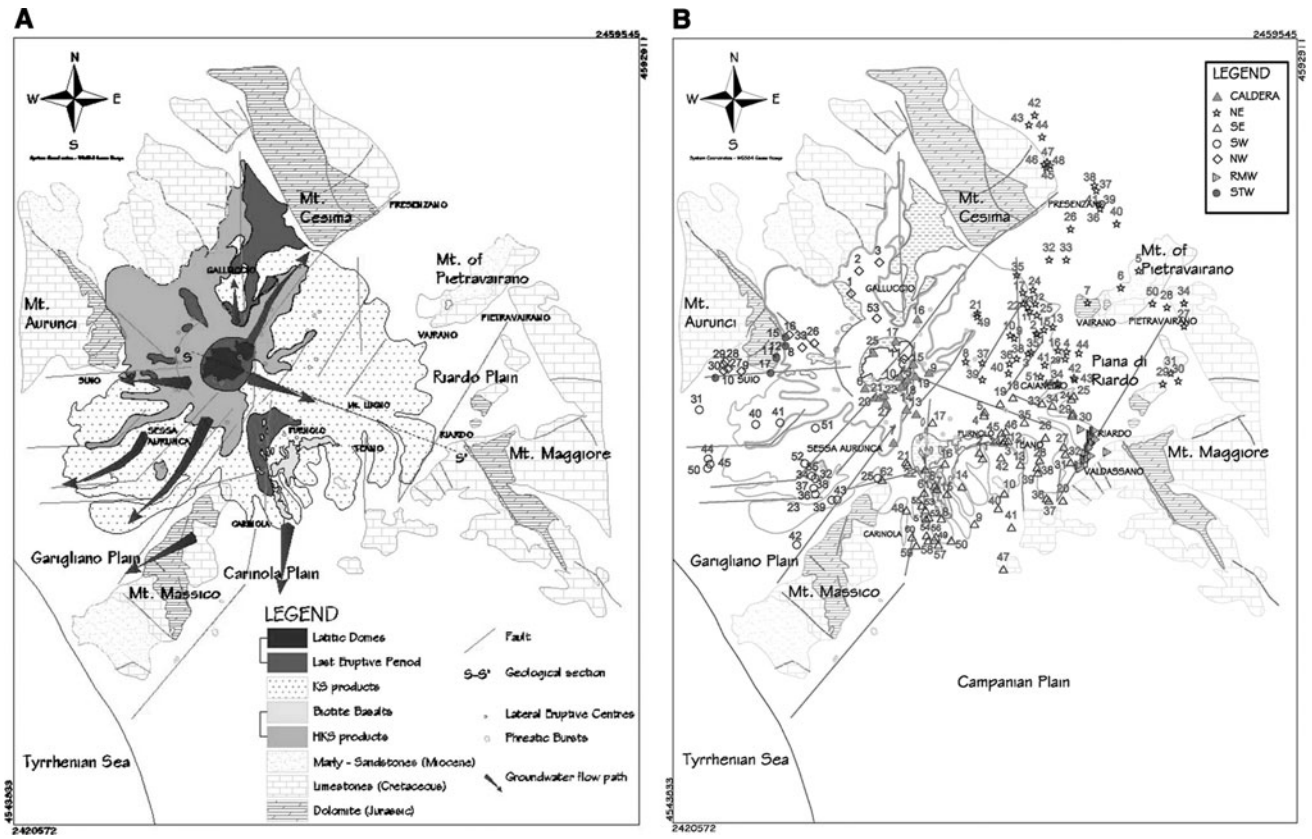

Fig. 1 **a** Roccamonfina volcano complex: General Volcanological and Geological Map, modified from De Rita and Giordano (1996). **b** The Roccamonfina sample location points. Groundwater flow paths are described by *arrows*

the massive Mesozoic carbonatic layers. Several discontinuities allow direct contact with the carbonatic basement and the oldest Roccamonfina lavas (Capelli et al. 1999). Carbonate and marl horsts surround the volcanic edifice.

The magmatic evolution of the RVC is characterized by variations in SiO_2-saturation and K content, i.e., the KS potassic series and the high-K series, HKS (Appleton 1972; Peccerillo and Manetti 1985). The compositional differences occur as consequence of partial melting of a metasomatized K-rich mantle source (Wendlandt and Eggler 1980). The first eruptive period resulted in the emplacement of high-K series (hereafter HKS) tephrite-phonolite stratocone, which outcrops in the W-NW sector of the volcano (Fig. 1). The stratocone is highly eroded and contains numerous shallow ravines. Leucite dominates the silica under-saturated HKS rocks that have evolved from leucite-tephrites to leucite-phonolites. Clinopyroxene and minor olivines are the dominant mafic minerals, while sanidine and nepheline are often present in the groundmass of more evolved rocks, such as leucite-phonolites and leucite-tephriphonolites. Melilite is present in the primitive, strongly silica under saturated rocks. Biotite, amphibole, and melanite are found in the differentiated rocks (Gambardella et al. 2005).

The end of HKS period results from the discharge of the HKS magma reservoir during KS magma recharge contemporaneous with eruption and emplacement of the BLT. The BLT was emplaced within a morphological depression on the SE side of the volcano (Luhr and Giannetti 1987; Cole et al. 1993). The White Trachitic Tuff (WTT), emplaced around the volcanic edifice, is the product of the major KS eruptive phase (Giannetti and Luhr 1983; Ballini et al. 1989; Giannetti 1990; Valentine and Giannetti 1995). The WTT consists of white and gray trachytic pumices (Giannetti and Luhr 1983) with few lythic accumulation zones (Giannetti and De Casa 2000). The termination of KS period is marked by the emplacement of two effusive, strombolian, latitic domes: the Lattani and the S. Croce domes (Rouchon et al. 2008). The final stages of RVC activity consists of localized phreatomagmatic eruptions that led to the production and emplacement of the Yellow Trachytic Tuff (YTT) from the N flank of the volcanic edifice, which result in the maar–shape of the northern crater (Giannetti 1996).

Hydrogeological setting

The connection between the RVC volcanic sequence and the sedimentary basement allows transmission of groundwaters from a limited spatial extent through the low and impermeable multilayer aquifer system (Allocca et al. 2007). The hydrogeological system was first described by Capelli et al. (1999), while the groundwater flow path dynamics were characterized by several authors (Allocca et al. 2007; Capelli et al. 1999; Celico 1983). Lava flows and domes are highly permeable because of extensive permeability along cooling generated fractures. Likewise, breccias are highly permeable and in direct contact with the sedimentary basement (Watts 1987). Groundwater recharge into the system occurs along dip-slip faults through the lava domes (Capelli et al. 1999). Conversely, pyroclastic formations act as barriers to groundwater flow because of their welded texture. Pyroclastic formations result in variable extent and thickness for permeable layers and confine the zones where the aquifer is recharged.

A carbonate regional aquifer recharged from the lateral Apennine chain reservoir is the basement of the RVC. The carbonate aquifer is highly permeable because of long-term chemical weathering and karstification. Groundwater transport within the carbonate regional aquifer is discontinuous because of localized impermeable clay/marl complexes interposed between the carbonatic basement and the lavas of Roccamonfina first eruptive period. Moving away from the volcanic edifice, the carbonate sedimentary basement is overlain by pyroclastic deposits and highly permeable, unconfined detrital material, which leads to variations in groundwater transport (Allocca et al. 2007).

Endogenous CO_2 emissions in cold groundwaters within the region are common, with the most famous example in Italy located in the Riardo plain. Other CO_2 springs such as those located NW of RVC nearby Suio (Fig. 1) have markedly different physicochemical parameters. In CO_2 spring near Suio we find the highest water temperatures in the area. At a first approximation, the location of mineral-gas rich springs and RVC relate to the regional tectonic setting and indicate that faults control the location of CO_2 emissions.

On a regional scale, groundwater transport occurs along radial flow paths (Fig. 1) with typical centrifugal water circulation from the central part of the crater to the surrounding plain (Allocca et al. 2007). In the SE sector of the volcano, the unconfined and semi-confined aquifer of RVC flows into the Riardo Plain and the lower Volturno Plain. In addition, groundwaters discharging from the southern side of Mt. Maggiore significantly contribute to the Riardo Plain aquifer. In fact, Mt. Maggiore is considered a separate hydrogeological system from the Riardo Plain, discharging into the deepest aquifer of the Volturno Plain (Capelli et al. 1999; Celico et al. 1977, 1980; Corniello 1988a, b).

Materials and methods

The current study includes 206 samples from six primary areas with the RVC (Fig. 1b). Sampling areas include:

the Caldera, NE, NW, SE, SW sides of the volcano, and the Riardo Mineral Waters (RMW), respectively. Samples include water obtained from irrigation wells, drinking water wells, and natural springs. Water temperature, pH, and conductivity were measured during collection in the field. All sampling materials were pre-washed with ultra-pure Q grade Millipore water and stored in PE flacons.

Major elements were analyzed by ion chromatography (Dionex DX-120) on unfiltered (F^-, Cl^-, Br^-, NO_3^- and SO_4^{2-}) and filtered (Na^+, K^+, Mg^{2+} and Ca^{2+}) samples. Alkalinity was measured by in situ titration with 0.1 N HCl acid using methyl orange indicator. Samples collected for metal analysis were filtered in the field using 0.45 μm Millipore MF filters and acidified (~2%) with ultra-pure HNO_3. All sample analyses show a charge balance error of less than 5%.

Minor and trace element analysis was carried out in the AMRA Laboratory using an Agilent 7500 ce ICP-MS ORS technology (utilizing collision cell technology). The following elements were analyzed according to the methods described by Wilbur and Soffey (2004): Li, Be, B, Al, Si, V, Cr, Mn, Fe, Co, Ni, Cu, Zn, As, Rb, Sr, Mo, Ag, Cd, Sb, Cs, Ba, La, Eu, Ho, Yb, Tl, Pb, Th, U. Internal standards Y and Tb were used to monitor for instrumentation drift. External precision was monitored using proper spike standard, which indicates errors of less than 5% for all analytes reported. The analytical results have been reported in Table of electronic supplementary material (ESM). For giving indications in the text regarding the distribution of chemical variables, the mean value, min, and max of each measured parameter have been reported in Table 1.

The Principal Component Analysis (PCA) has been used in this work to summarize the whole chemical (and physical) information of our data set. Often, for geochemical data, several variables are highly correlated, reflecting relatively few underlying mechanisms which drive natural processes. In PCA, this correlation between different variables is used to find principal components (PCs) (Massart et al. 1988). The results of this elaboration can then be reported on a scatter diagram of "factor scores" for each variable. In fact, variables governed by a similar hydrogeochemical process plot close to each other and obviously far away from variables affected by a significantly different natural and/or anthropic process. The use of multivariate techniques to search for structure in geological and hydrochemical data has been deeply discussed and described by Joreskog et al. (1976), Davis (1986), Reyment (1997) and Buccianti (1997). The PCA has been carried out with Statistica 6.0 software.

Table 1 Mean value, min and max of each measured parameter

	Caldera	RMW	SW	SE	NE	NW	STW
T (°C)							
Min	12	17	15	13	15	13	29
Max	16	20	25	26	29	22	49
Mean	14	19	17	18	20	18	40
pH							
Min	5.2	5.7	6.4	5.1	5.9	4.9	5.8
Max	7.2	7.5	7.3	7.3	7.8	8.3	6.6
Mean	6.5	6.1	6.9	6.4	6.7	6.8	6.2
EC (μS/cm)							
Min	134	416	261	236	186	176	1,273
Max	326	3,519	896	863	1,736	864	3,650
Mean	215	1,780	501	406	495	464	2,560
HCO_3 (mg/l)							
Min	46	204	101	57	57	62	1,434
Max	184	2,855	541	500	1,167	592	2,258
Mean	83	1,265	218	167	232	211	1,705
F (mg/l)							
Min	0.1	0.6	0.5	0.1	0.04	0.1	1.2
Max	0.39	1.3	3.4	3.9	270.9	2.8	4.4
Mean	0.1	1.1	1.5	0.7	8.1	1.2	2.3
Cl (mg/l)							
Min	7	12	12	11	0.2	9	36
Max	19	32	45	43	133	42	333
Mean	13	20	29	21	18	16	126
Br (mg/l)							
Min	0.03	nd	0.03	0.01	0.01	0	0.02
Max	0.03	nd	0.18	0.12	38.9	0.2	1.05
Mean	0	nd	0.07	0.05	1.9	0.05	0.45
NO_3 (mg/l)							
Min	0.6	0	0.02	0	0.03	0.03	0.1
Max	21.2	12.1	92.7	106.2	73.6	82.8	1.0
Mean	6.5	5.9	20.0	15.0	20.8	10.5	0.5
SO_4 (mg/l)							
Min	2	1	3	3	2	1	144
Max	19	6	52	56	77	78	435
Mean	7	4	14	13	17	22	223
Na (mg/l)							
Min	7	25	16	12	4	7	49
Max	15	87	50	63	87	42	367
Mean	11	49	31	27	20	19	150
K (mg/l)							
Min	3	21	10	3	1	0.1	17
Max	26	86	58	47	50	61	103
Mean	7	43	34	20	12	23	52
Mg (mg/l)							
Min	3	3	4	4	3	2	109
Max	7	61	39	22	38	53	206
Mean	5	22	11	10	10	11	139

Table 1 continued

	Caldera	RMW	SW	SE	NE	NW	STW
Ca (mg/l)							
Min	10	31	9	11	9	9	312
Max	25	706	110	112	299	128	542
Mean	17	327	35	28	57	33	384

	Caldera	RMW	SW	SE	NE	NW
Li (mg/l)						
Min	1	25	2	1	nd	2
Max	14	193	36	69	24	54
Mean	3	81	22	17	8	17
B (mg/l)						
Min	4	63	51	18	4	13
Max	47	1,106	201	265	454	167
Mean	22	406	86	74	50	76
Al (mg/l)						
Min	0.2	1	3	0.1	nd	4
Max	26	69	23	657	130	314
Mean	13	23	13	83	15	73
Si (mg/l)						
Min	9	37	11	nd	4	16
Max	34	60	39	41	39	56
Mean	18	47	28	33	23	34
V (mg/l)						
Min	7	1	6	0.3	0.3	5
Max	37	21	60	37	41	23
Mean	15	11	21	13	8	14
Mn (mg/l)						
Min	2	1	0.1	0.1	0.2	0.2
Max	93	851	25	1804	54	933
Mean	48	225	6	176	6	187
Fe (mg/l)						
Min	1	3	28	0.2	0.2	23
Max	14	5,277	685	22710	186	25
Mean	9	1,063	234	2580	24	24
Zn (mg/l)						
Min	4	1	0.1	0.4	3	2
Max	59	25	1,181	24,915	6,406	327
Mean	18	8	145	823	315	66
As (mg/l)						
Min	7	3	1	nd	1	2
Max	11	40	22	120	25	20
Mean	9	10	7	7	9	11
Rb (mg/l)						
Min	8	57	11	17	nd	6
Max	44	209	61	183	233	422
Mean	25	125	31	57	44	117
Sr (mg/l)						
Min	89	101	67	83	19	36
Max	386	1,666	403	396	1,249	1,369
Mean	195	644	153	214	294	345
Ba (mg/l)						
Min	2	nd	0.3	nd	0.3	1
Max	35	243	19	127	177	22
Mean	12	65	4	12	32	7
U (mg/l)						
Min	nd	0.1	1	0.1	0.1	1
Max	nd	4	21	23	24	33
Mean	nd	2	8	3	4	10

Results and discussion

Chemometrics

Results of the PCA for all chemical and physical parameters are reported in the ''factor scores'' scatter diagram of Fig. 2. The first factor explains 31.9% of the total variance and the second the 14.6%. Most of the correlations are related to water–rock interactions, and from the study of the factor scores scatter diagram is possible to locate different groups of variables. Each group should describe a specific hydrogeochemical process. For example, the mineralization degree is related to the Electric Conductivity (EC), the Ca-HCO_3 (carbonates), and the K–F–B (volcanic) elements. The result is important, because it shows that parameters belonging to different geological facies, sedimentary (carbonates), and volcanic (lavas or pyroclastic) are representative of the water–rock interaction in RVC. Hydrothermal processes, such as those of Suio thermal springs, are detected by the correlation of Temperature-SO_4–Cl–Na–Mg. This association provides information on the occurring of intense water–rock–gas interactions in the shallow hydrothermal system. This process results to be different from that bringing at surface of Riardo and Teano CO_2-rich waters, where despite the high gas flux, water temperature is cold (Table 1, ESM). Minor elements show a statistical result similar to that of major ions. Their distribution is also based on water–rock interactions. For example, it is worth noting that Sr and Ba are found in both carbonatic and volcanic rocks (Tesoriero and Pankow 1996), and then their correlation is a consequence of a similar geochemical behavior, although in different geological contexts, during water–rock interactions. Similarly, Rb and Li seem to be associated only to waters flowing into volcanic rocks. At the most lower-right side of Fig. 2 there are parameters (most of them redox sensitive) generally associated with water-volcanic rocks

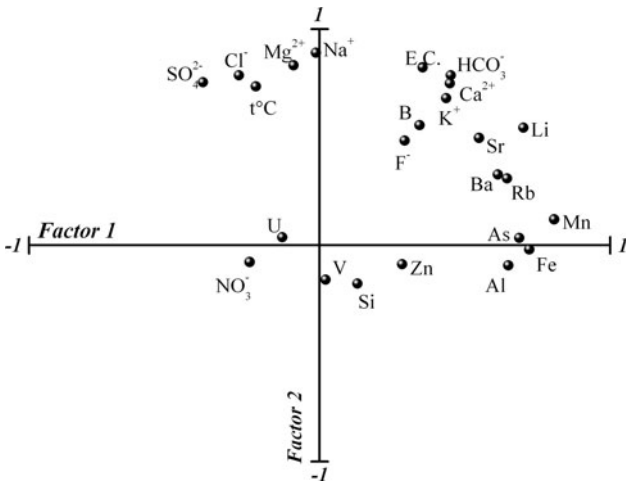

Fig. 2 The Principal Component Analysis (PCA) on the measured chemical variables. The first factor explain the 31.9% of the total variance while the second the 14.6%. From the study of factor scores scatter diagram it is possible to find the variables group that best describe the different characteristic hydrogeochemical processes (see text)

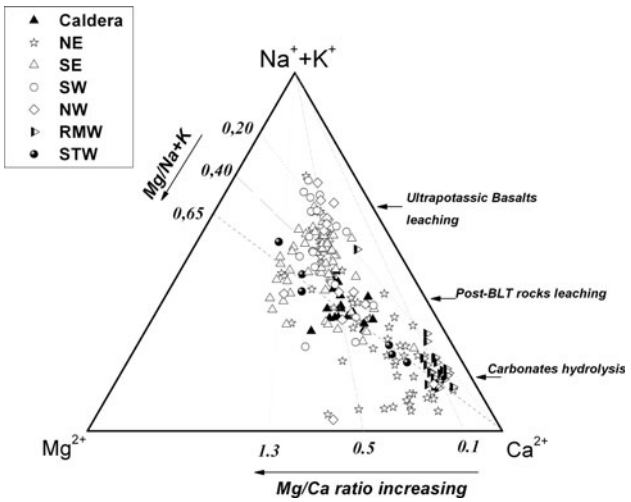

Fig. 3 Major metals triangular plot. Specific trends and values are *highlighted* to show different hosting litotypes interactions and characteristic ratios

interactions. These variables are divided into two subgroups: (V–Si–Zn) and (Al–As–Fe–Mn). We find a high correlation between V and Si from one group and Al, As, Fe, Mn on the second, with a high R-Pearson coefficient from 7 to 8.5 in groundwaters circulating in volcanic—effusive rocks (i.e. caldera's wells and mineral springs). Conversely, this correlation is not likely to occur in groundwaters having carbonatic features. Finally, the last correlation to be taken into account is between NO_3 and Uranium.

Water–rock interaction

The ternary diagram of Fig. 3 shows the relative concentration of major cations. The position of sample points on the plot indicates water–rock interaction processes. The sample distribution highlights a large spatial variation due to different hydrogeochemical dynamics which can be explained using the Mg/Na + K, and Mg/Ca ratios (meq/l). The hydrogeological features discussed in "Geological setting", allows us to propose the influence of carbonates on groundwater chemistry at the periphery of the volcanic edifice. In fact, a low Mg/Ca ratio of 0.1 is characteristic of $CaCO_3$ due to calcite dissolution (Celico 1988). This process preferentially leads to calcium enrichment compared to Mg. Conversely, the increase of Mg (compared to Ca) is indeed a direct consequence of water interaction with MgO-rich rocks, such as volcanics (basalts).

As shown in Fig. 3, the RVC characteristic Mg/Ca ratio could be assumed to be ~0.5 if we except few samples (From SE14 to SE19) showing a Mg/Ca ratio from 1 to 1.3 with an increase of Mg (from 10 to 22 mg/l) versus Ca concentrations ranging between 10 and 20 mg/l. This Mg/Ca shift is also associated with a K decrease (from 15 to 3 mg/l).

The first group of samples is placed on top of Fig. 3. It shows the lowest Mg/Na + K ratio, with a value of 0.2 and with the characteristic Mg/Ca ratio at RVC of 0.5. This chemical facies is representative of groundwaters hosted in the Roccamonfina first period lavas. Most of the collected samples belong to the NW and SW sides and few others from the NE side of the volcano. These samples show ultrapotassic (water-HKS rocks interaction) chemical features. They must belong to the tephritic aquifer belonging to the first eruptive period. At the SE side and mainly from the NE side of the volcano, the pyroclastic rocks (related to the second explosive activity period) show a relative chemical variation of the hosted water. The Mg/Ca ratio remains almost unchanged (0.5) and, in agreement with the variation of the chemical composition of volcanic tuffs, compared to the products of the first period lavas, the Mg/Na + K ratio increases from 0.20 (HKS-basalts interactions) to 0.40 (water–tuffs interactions). The caldera groundwaters show a progressive K-decreasing trend as a consequence of the influence of the latite domes on groundwaters. Latite domes belong to the last eruptive period of the RVC and are originated from the most differentiated magma, with the highest CaO and MgO Wt% and the smallest K_2O Wt% compared to trachytic and tephritic products belonging to first and second Roccamonfina eruptive periods (Paone 2004). Therefore, most of the intracaldera groundwater samples show an Mg/Na + K ratio from 0.4 to 1. Finally, the Mg/Ca ratio decreases from 0.5 to 0.1, showing the shift from volcanic to carbonate

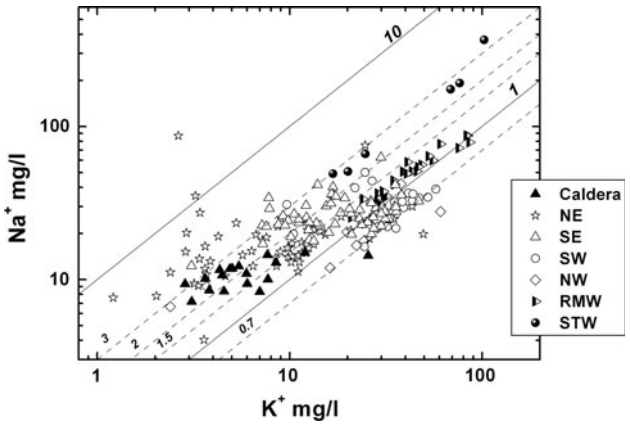

Fig. 4 Na/K specific ratios have been shown. Groundwater hosted in ultrapotassic aquifer shows a value of 0.7 with a gradual shift from 1 to 3 with samples hosted in second eruptive period rocks. Carbonate waters of the neighboring plain, which are not influenced by Roccamonfina volcanic waters mixing, show the highest ratio (10)

dissolution in the sampled groundwaters. Samples characterized by this process are those closely located to the Ca corner in Fig. 3. Chemical differences between RMW samples with those collected at the base of the NE side of the volcano using the Na/K ratio are reported in Fig. 4. The Na/K ratio is a key parameter to distinguish the carbonate-sedimentary from volcanic (high-K) rock's influence on groundwaters flowing in these lithologies. In fact, the Na/K ratio close to 1 is typical of alteration processes in silicate–volcanic rocks of the Campania-Lazio volcanic areas (Chiodini and Frondini 2001). At Roccamonfina volcano, waters interacting only with the ultrapotassic rocks show a similar Na/K ratio of 0.7.

Conversely, Na/K ratio of about 10 with an Mg/Na + K > 1 found at Pratella, Presenzano, and Vairano (NE, Fig. 1) waters suggests that the aquifer is exclusively hosted into carbonate formations and do not receive groundwater recharge from the volcanic edifice. This is evident from the cluster of samples in the lowest part of the triangular plot in Fig. 3. Differently, shallow Roccamonfina groundwaters flowing in the surrounding southern plains mix with local groundwaters coming from neighboring carbonate reliefs. Such a dynamics has been detected at the periphery of Teano area (SE10, SE4) at Carinola and Piedimonte Massicano plains (SW42).

However, groundwaters from Teano and Riardo plain also showing bicarbonate-alkali earth facies are characterized by a very different chemical composition.

These latter areas are characterized by supersaturated CO_2 waters with a high mineralization and a bicarbonate alkali-earth *facies* suggesting a CO_2-carbonate interaction and dissolution. Conversely, waters collected within the carbonate aquifer at a depth of 200 m or more show a Na/K ratio between 1 and 1.5 (Fig. 4). We conclude that the RMW are supplied by waters flowing within both volcanic and carbonate formations. Similar features are typical of the "Acqua Calena" sample (SE47) located within the prolongation of the Valdassano fault, at the NW foot of the Francolise carbonate hill (Fig. 1). Hydrogeochemical dynamics showing similar chemical evidences has been also detected along the Savone creek nearby the Teano town. Samples SE2, SE3, SE5, SE7, and SE46 (the mineral waters of the Caldarelle spring) located in the middle of the Roccamonfina SE side, show a Ca-rich phase due to the addition of waters from the deepest water reservoirs. It has been found that most of these evidences are obtained on samples located along a specific tectonic alignment (Fig. 1). The presence of gas-rich springs is often associated with lateral/peripheral volcanic activity, as shown by the presence of M. Lucno, one of the several Roccamonfina lateral eruptive centers. Therefore, at the SE side of the RVC and within the Riardo plain, faults seems to be the main pathway for deep groundwaters (and gas emissions) to come to surface. Springing of groundwaters from the deep aquifer has been related to Ca and EC increase, and Na/K ratio decrease (1–1.5) due to the simultaneous presence of HKS basalts and carbonate within the volcano basement.

To estimate the residence time of waters in the aquifer of the Roccamonfina, chloride concentration, as suggested by Celico (1988), should be the parameter to be used. It is clear that groundwater mineralization increases with the rising distance from the point of origin. In our area, mineralization is maximal in the lower part of the volcanic edifice where mixing between volcanic and carbonate groundwaters occurs.

A different correlation line between Electric Conductivity and chloride occurs when groundwaters circulate into different litotypes. The correlation shown in Fig. 5 confirms the suggestions of two linear correlation functions. The first one (line A) highlights the water–volcanic rock interactions from within the caldera to the feet of the Roccamonfina volcanic edifice, while the second correlation function (line B) shows the carbonate water samples (Pietravairano, Pratella and Presenzano) and the CO_2-rich samples of the RMW, and Teano (SE side). This trend confirms the influence of carbonate rocks involved in the mineralization processes of mineral waters (e.g. RMW). The geothermal area of Suio shows thermomineral springs located in a boundary zone between the RVC's NW side and the Aurunci carbonatic range. The chemical composition of these springs reflects the unique lithology (e.g. "Hydrogeological setting") of the aquifer where they are flowing. From Figs. 3, 4, 5 it is clear that the volcanic versus carbonatic *facies* suggests that mineralization is strongly enhanced by acid gas emissions (CO_2, H_2S) and high temperatures. The intense water–rock interaction in

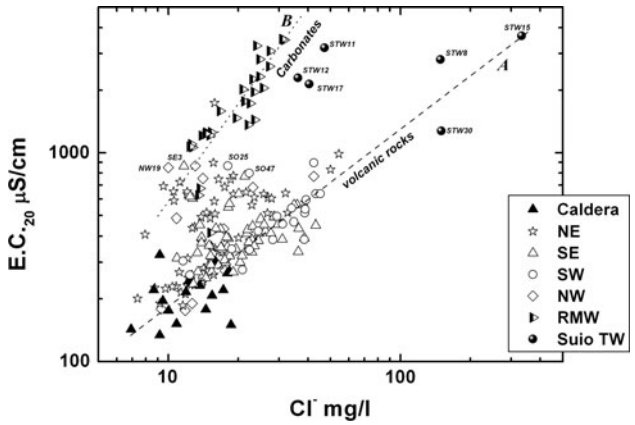

Fig. 5 Correlation between the normalized electric conductivity (E.C.) and chlorine is indicative of groundwater residence time and/or water–rock interactions. The two different alignments clearly separate groundwaters hosted exclusively in volcanic rock from those mainly interacting with carbonate during their flow path

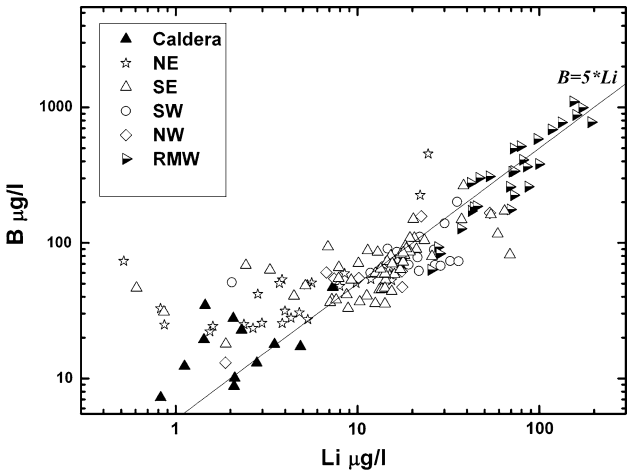

Fig. 6 B/Li ratio. Calculated regression line gives the equation: $y = 4.8x + 8.1$ with an R equal to 0.92. Constant ratio value and a very high correlation degree of these two parameters characterizes the value of the RVC groundwaters, despite of different ages and type of erupted rocks

such a structural bordering zone brings, as a final product, high mineralized waters whose chemical composition strictly reflects the host rock lithology.

Diagnostic minor element distribution

Leaching of volcanic rocks

Analytical results and the associated statistical treatment show that boron and lithium have a linear correlation with an R-Pearson of 0.92 (Fig. 6). Enrichment of lithium depends exclusively on interactions of groundwaters with volcanic rocks as confirmed by the very low concentration of this element in pure carbonate groundwaters, e.g., nearby Pratella-Presenzano area (Table 1, ESM). Most of the collected samples cluster close to a B/Li ratio of 5 (Fig. 6). The linear equation reported in the same figure highlights that B and Li are in a fairly constant ratio in groundwaters, independently from the different volcanic products and ages of Roccamonfina. It is worth noting that bicarbonate–alkali earth elements at RMW show the highest B and Li content compared to all others RVC samples. This is considered to be a direct consequence of the RMW initially originating from Roccamonfina volcanic rock dissolution.

In order to explain such a dynamics, it can be of some help to describe the Mg versus Li correlation. Pre-treatment statistical data give a weak (0.31) Mg–Li R-Pearson coefficient for the whole data-set. However, if the same operation is repeated on different samples subgroups of the western flank of the volcanic edifice (e.g. SW and NW, where products of the first period lava is the predominant aquifer's lithology, Fig. 1), it gives an extremely high R of 0.95. The Mg/Li ratio shows a linear constant value of about 0.25 (ppm/ppb) for samples located within the first eruptive period lavas and, more generally, at RMW area.

Differently than in first period high-K lavas, low Mg–Li correlation is found for groundwaters circulating in the second and third eruptive period products, e.g., the majority of samples collected within the eastern flank of the volcanic edifice. While only few samples of the SE side show similar chemical characteristics to the RVC first period eruptive products, with a Mg/Li ratio value close to 0.25, the majority of SE samples show a much higher ratio with contents of Mg and Li varying between 3 and 20 (ppm) and 0 and 20 (ppb), respectively. At the SE side of the volcano two different groundwaters have been collected in the first period lava. The first groundwater is located within a superficial aquifer between Casale di Carinola and Teano where rich-biotite basalt outcrops (Fig. 1). These groundwaters (e.g. SE2, SE11, SE55, SE53) show the same Mg/Li ratio of the deepest and most mineralized wells of RMW. The second type of groundwater is related to a deep aquifer hosted in the HKS lavas of the area. We found this chemical feature associated with several samples: (1) mineral springs (SE46, Caldarelle) and deep wells CO_2-rich located along the NW–SE fault of the Savone bed (SE3, SE4) and ii) wells placed along Valdassano fault line (SE20, SE29) and the Acqua Calena mineral spring (SE47).

From alkaline to alkali-earth groundwaters: carbonate chemical influence, riardo mineral water dynamics

From the previous section and the possible physical and chemical processes occurring in this area, we have shown that waters flowing from the volcanic edifice mix with

carbonate groundwaters and/or flow directly within the outcropping carbonate lithotypes. This process is recorded through the enrichment of alkali-earth ions. Such a dynamics is confirmed by the shift of collected waters toward the Ca corner in the triangular plot of Fig. 3. From a careful data analysis, as expected, Strontium and Barium enrichment are then the direct consequences of water–carbonate rock interactions. The Ba/Ca and Sr/Ca ratios (expressed as ppb/ppm) give important information related to groundwater mineralization on the eastern flank of the volcanic edifice. The different Ba/Ca ratios can discriminate water interactions with carbonates versus those occurring with volcanic rocks. As shown in Fig. 7, the Ba/Ca ratio has two (very different) reference values, 1 and 0.05. We will assume these values as characteristic of groundwaters flowing within (1) pure carbonates and (2) pure volcanics, respectively. In fact, rich-alkaline earth waters from Pratella, Presenzano, and Vairano have a Ba/Ca = 1, while volcanic/alkaline waters from the SE side of Roccamonfina volcano show a typical value of 0.05 (Fig. 8b). Intermediate value of ~0.25 can be likely interpreted as a mixing of different waters and/or as a single water interacting with both litotypes : (1) volcanic groundwaters intersecting neighboring carbonate rocks and/or carbonate groundwaters. A second mixing process (2) occurs at depth, along fault lines where important CO_2 fluxes allows (deep) mineralized carbonate waters to mix with (superficial) volcanic groundwaters.

Figure 8 shows the Sr/Ca ratio distribution. The Ca-rich waters originating within carbonates are responsible for the decrease of the Sr/Ca ratio from 10 to 2, where (at RMW springs) the strongest Ca input takes place.

Our results combined with the hydro-geological and stratigraphical data of the area (Capelli et al. 1999) allow proposing a new schematic model (Fig. 9) for groundwater flow path at the SE side of the volcanic edifice. The model allows understanding the interactions between deep and shallow groundwaters and the recharge of the deep, carbonate aquifer of the Riardo Plain. As shown in Fig. 9 the recharge of the Roccamonfina volcano deep aquifer occurs with the direct infiltration of rain waters within the caldera ("Hydrogeological setting"). Groundwaters will first flow through deep basaltic-HKS and then run into the Riardo plain within deep carbonatic aquifers. This water path is confirmed by the absence of lavas in the stratigraphy of the Riardo Plain. In fact, it is worth noting that chemical elements, characteristic of water-volcanic rock interactions, such as alkali metals, silica, Fe, Mn, and As, are strongly enriched in groundwaters collected within the confined Riardo Plain carbonate aquifer. Finally, we can propose that the RVC deep lava aquifer is likely feeding the carbonate aquifer of the Riardo Plain. In fact, the RMW show both volcanic and carbonate features as consequence of

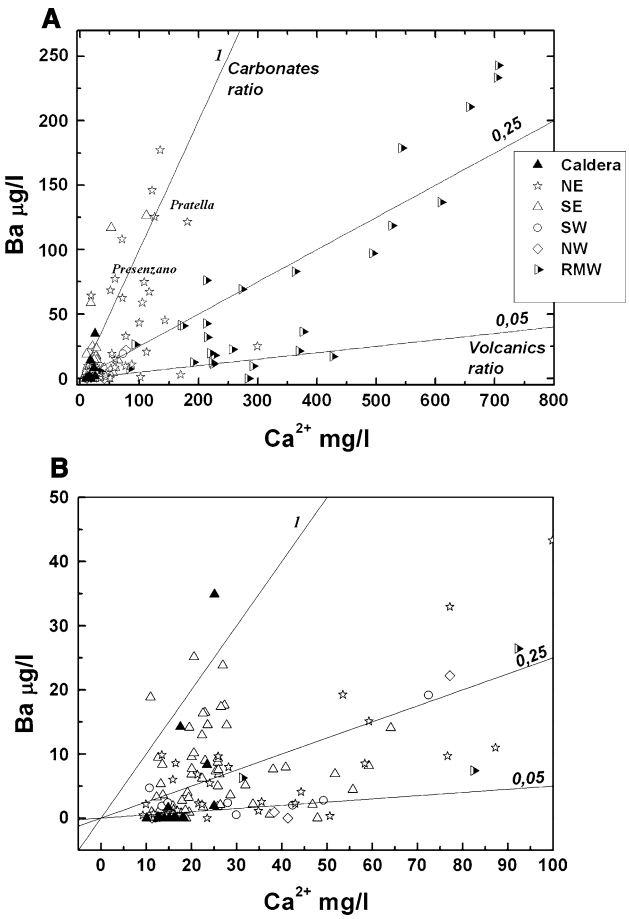

Fig. 7 **a**, **b** Calcium and Barium are alkali earth elements enriched in carbonates waters. The Ba/Ca ratio highlights the different waters mineralization steps (see text) of Presenzano and Pratella in comparison with the deep one occurring at Riardo Mineral Waters

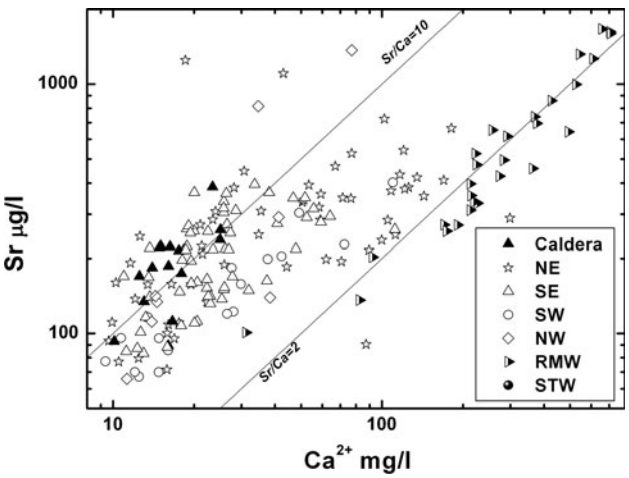

Fig. 8 Due to Ca enrichment as a direct consequence of carbonate alteration, the Sr/Ca ratio strongly decreases from 10 to 2 at RMW springs where the highest Ca input takes place. A fair correlation is found with the EC_{20} − Cl (as reported in Fig. 5)

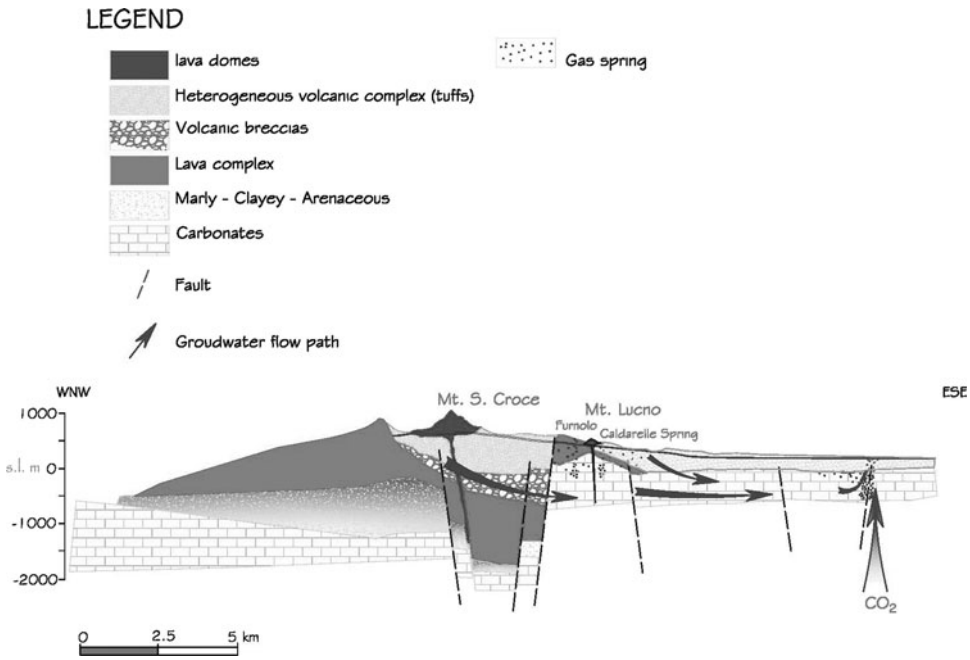

Fig. 9 Schematic section of SE groundwater deep circulation and Riardo mineral water recharge and mineralization. Stratigraphical data are from Capelli et al. (1999)

two-type mineralization processes, obviously occurring in two different moments. The first mineralization occurs at depth, beneath the Roccamonfina volcano where waters flow into lava formations bringing in solution alkaline elements and silica, while oxygen is consumed allowing Fe solubilization as Fe(II). At the end of this process these same waters run into the Riardo Plain carbonate aquifer. The second mineralization step occurs along the Valdassano fault where high fluxes of CO_2 coupled with high-mineralized deep carbonated waters mix with those slightly more superficial flowing from the Roccamonfina volcano (Giordano et al. 1995). This process is shown from Figs. 3 to 8 by the perfect linear correlation among all chemical parameters at RMW. The CO_2 fluxes are responsible for intense carbonate hydrolysis bringing in solution large amounts of alkali-earth metals. These waters have a marked bicarbonate alkali-earth feature deviating from all typical ratio values of Roccamonfina waters compared to Ca, Sr, and Ba (Figs. 7, 8). This model is also confirmed by the long residence time, in the order of 25 years, calculated by Tritium measurements (UT) in some Riardo mineral springs (Celico et al. 1980). These data confirm that deeper and more mineralized RMW have a very slow flow path and take almost 25 years to travel from the Roccamonfina water table up to the Riardo plain.

One more evidence of the deep carbonate hydrolysis at Riardo Plain is the buffer capacity against the CO_2 acidification of deep groundwaters. In Fig. 10 it is possible to clearly distinguish the RMW from those belonging to RVC. The latter have subacid pH likely due to water circulation within the volcanic aquifer, which is also confirmed by the slight HCO_3^- enrichment. On the other hand, along the Valdassano fault in the Riardo plain, CO_2 degassing is responsible water acidification coupled to a bicarbonate increase. These conditions favor carbonate hydrolysis at depths of 200 m and more; however, here a reversal trend of acidification due to the $CaCO_3$ buffer activity also occurs. It is worthy to note that the same phenomenology occurs at the Suio thermal waters, located at the opposite side, although here waters flow from carbonates instead of volcanic rocks.

Hydrogeochemical processes at the western side of Roccamonfina Volcanic Complex

Suio thermal waters (western side) show chemical differences from mineral waters of the Eastern side. Both mineral waters are considered soda springs (Giggenbach 1988), in other words, the chemistry of both mineral waters depends on water-hosting rock interactions. The Suio thermal waters could be divided in two sub-groups according to the amount of solubilized $CaCO_3$ or, similarly, to the degree of interaction with carbonatic rocks. Figures 3 and 4 show that all Suio thermal waters have a very similar Mg/(Na + K) and Na/K ratio (0.65 and 3, respectively) confirming their circulation into the same type of volcanic deposits of the western flank of the volcanic edifice. However, a portion of this thermal basin shows also evidence of interactions with carbonatic rock (e.g. STW2, STW3, STW5) of the Aurunci range (Fig. 1).

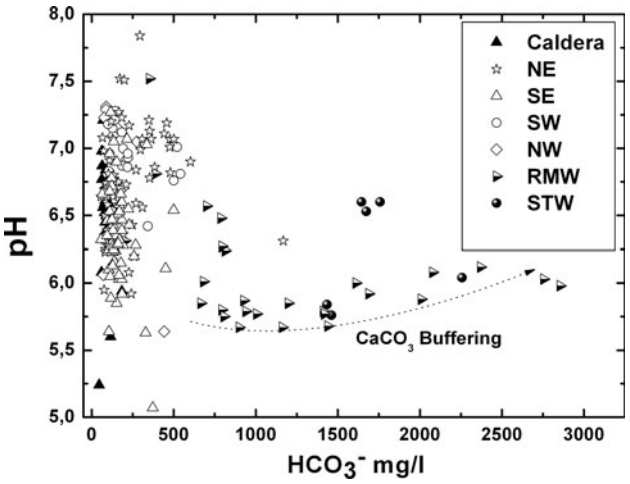

Fig. 10 CO_2 addition to groundwaters is the main factor decreasing the pH. It is possible to distinguish between alkaline groundwaters ("volcanic waters") on the left side of the figure and the alkali-earth groundwaters which are the richest in HCO_3^-. The intense, "in situ", mineralization nearby the Valdassano fault (deep Riardo mineral waters and Riardo plain carbonate aquifer) brings in solution large amounts of $CaCO_3$ with the CO_2 buffering effect and giving to the pH-CO_2 a reversal trend. The same process occurs in the thermal-carbonatic springs of Suio

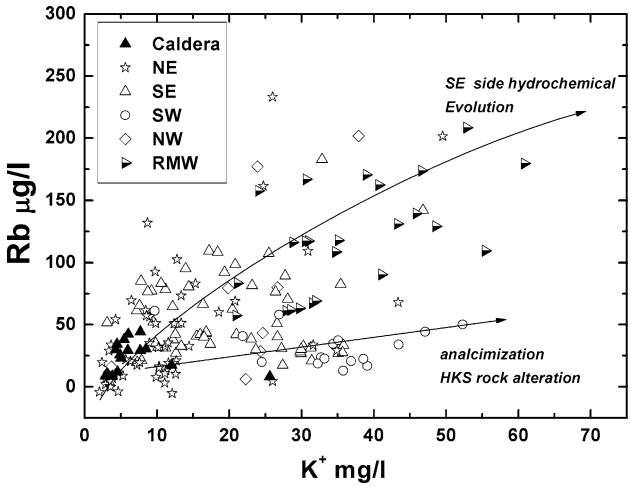

Fig. 11 As proposed by Giannetti and Masi (1989) the leucite analcimization brings to K enrichment in the circulating solutions while retaining Rb. Our data confirms such analcimization process. In fact the Rb/K ratio of samples hosted in Leucitic Tephrite (HKS or in basalts in general) show a lower Rb/K ratio than those groundwaters belonging to volcanic products erupted during the last eruptive period

As previously explained, the Suio thermal waters show the highest temperature of the whole studied area, associated with the highest SO_4^{2-} and Cl^- contents (Fig. 5).

Another geochemical process to be highlighted is related to the Rb distribution in cold groundwaters. Giannetti and Masi (1989) studied the analcimization process during leucite weathering. The result of the above study highlights that during HKS basalts-leucite alteration, K is systematically trapped in the circulating fluid, whereas Na increases in analcime relative to leucite. This process is confirmed in our samples by the lowest Na/K ratio (0.7) of sample points hosted in the first period lava in the western flank of the volcanic edifice (Fig. 4).

One more result from Giannetti and Masi (1989) is related to the retention of Rb by analcime, and the consequent low (or lower) Rb content in the interacting waters compared to K content. Then Rb is considered to be more concentrated in the solid phase and less abundant in the circulating solution. Unfortunately, chemical analysis performed by Giannetti and Masi on water samples did not give satisfying results regarding this process. We have tried to compare our data with the previous process, studying the Rb/K ratio. Our chemical results agree with the Giannetti and Masi's (1989) hypothesis regarding Rb distribution between solid and liquid phases, as showed by Fig. 11. The Rb concentration in waters collected within the first period lava aquifer (samples located on the western side) show a lower Rb/K ratio compared to other samples hosted in different lithologies. The Carinola samples located at the SE side of Roccamonfina edifice shows a similar Rb/K ratio, likely because of the interactions with tuffs and basalts responsible for the groundwater chemistry. This is also confirmed by the high fluorine content from 1 mg/l in Carinola samples up to the 3–4 mg/l found on the western side and SE side deep wells, whose hydrogeochemistry only depend on basalts minerals weathering.

One last observation, always on Fig. 11, is related to the Rb concentration between eastern HKS deep groundwaters and similar (HKS) western shallow groundwaters. Deep groundwater samples show a larger Rb enrichment compared to shallow less-mineralized groundwaters. This finding likely occurs because of the thermodynamic difference occurring within deep and shallow aquifers in mineral alteration processes and for the different intensity of weathering processes.

Anthropogenic contamination considerations

The Roccamonfina volcanic groundwaters are traditionally well known as good quality drinking waters, and nowadays the whole area should be soon part of a new natural park project. In the studied area there are no big industries, although low/medium size activities dedicated to farm and/or zootechnic product processing are typical of this area. On the other hand, agricultural activities are historically widely practiced, chestnuts cultivations at greater heights while at the foot of the volcano, orchards and annual cultivars are produced. Our data (Table 1, ESM) shows a different degree of contamination. The heaviest has been localized in areas where population density is higher and

the productive activities more intense. The highest level of pollution (using as reference the nitrate concentrations) has been detected close or within urban centers and rural areas where a modern sewer system is lacking and often cesspits as waste water disposal systems are used. The correlation between nitrates and sulfates belonging to the whole data set gives a $R_{NO_3-SO_4}$ of 0.04. However, taking into consideration only samples with nitrate concentrations from 40 to 100 mg/l, the $R_{NO_3-SO_4}$ increases up to 0.80. This correlation highlights an important process related to sulfate distribution, and it shows that sulfur is related to two different sources. A natural one in Suio thermal waters, where high sulfur contents is not associated with nitrate increase. Here sulfates are associated with H_2S (gas) oxidation within thermal waters. Conversely cold Roccamonfina groundwaters usually show low-to-very low sulfates concentrations. The second sulfur source results from anthropogenic contamination, which is verified by the simultaneous increases in nitrate concentrations (r (SO_4 vs NO_3) = 0.9). Specific values of SO_4^{2-}/NO_3^- ratio can be assumed to be characteristic of particular human activities (Federico et al. 2004; Cuoco 2009). We can assume two end-members with associated indicative values: ~4 and 0.14, respectively. The SO_4^{2-}/NO_3^- of ~4 is characteristic of chemical fertilizers (N-rich sulfates) (Federico et al. 2004; Cuoco 2009). The second end-member, with a SO_4^{2-}/NO_3^- ratio of ~0.14 is considered to be related to waters coming from urban and rural sewages, animal waste, and septic tanks (Panno et al. 2001; Pawar and Shaikh 1995; Steinich et al. 1998). Our data are in agreement and confirm these findings.

Only a small portion of our samples (7%) exceeds the WHO limit of 50 mg/l of NO_3^-. These samples are located within the eastern plains of the volcanic edifice, i.e., Vairano and Caianello (NE2, NE4, NE7, NE12, SE25, SE30, SE5, SE40), and the separated basin of Presenzano (NE26, NE33, NE45). Similarly, on the western side of the volcano high NO_3^- contents have been found in nearby farms and urban centers (NW23, NW38, NW39), and at Galluccio (NW3). The highest nitrate concentrations associated with low S/N ratios suggests that contamination is related to an organic phase associated with sewage or farming wastes. A SO_4^{2-}/NO_3^- ratio between 1 and 4 is considered to be indicative of agricultural activity. Sulfate increase is likely due to S-rich fertilizers. These samples have also a high-nitrate concentration between 10 and 40 mg/l, suggesting a typical N–S-rich fertilizer.

In most cases the nitrate content is due to the synergic impact given by both fertilizers (with the highest SO_4^{2-} concentrations) and urban and farm waste (N-rich).

We have also found an unusual component in our samples, possibly related to the above-mentioned processes. Uranium is fairly enriched in our samples and seems to be related to the existence of a possible anthropogenic contamination. We observe varying U concentrations within the same sampling area and in different sampling areas. This finding suggests that U enrichment is unique to waters which experience considerable anthropogenic contamination (e.g. nitrates and sulfates).

Uranium seems then to be related to agricultural activity; in particular, it is associated with the use of phosphate fertilizers, which are very commonly used in this region. We have found that small U-contents are always present in these fertilizers and released into the environment where they are spread into soils (Lima et al. 2005). It has been recently suggested that different phosphate rocks contain variable concentrations of Uranium depending on the mining location (Al-Shawi and Dahl 1995). Then, sites where agriculture is well developed should be those were U-rich groundwaters are found.

Conclusions

The results obtained in this work are in agreement with the hydro-geological model recently proposed for the area (Allocca et al. 2007; Capelli et al. 1999).

Groundwater chemistry of the Roccamonfina volcano is characterized by a composite hydro-geologic dynamics and different mineralization processes related to different lithologies and CO_2-gas-rich emissions in the deepest water tables. The presence of deep active faults and the different stratigraphy from area to area of the volcano, and its environs are responsible for this process. Direct rainwater infiltration should be considered the main recharge from the central part of the caldera.

Chemical features can distinguish different groundwaters within and outside the caldera: (a) K-rich waters flowing between the ultra-potassic basalts related to the first eruptive period of Roccamonfina volcano. The aquifer should be considered superficial in the western part of the volcano and deeper on the eastern side. The eastern deep aquifer shows low redox conditions, presence of Fe(II), and evidences of carbonates hydrolysis, which is explained with waters continuously interacting with both volcanic and carbonate facies. Several springs belonging to the eastern side of the volcano show high CO_2-rich gas emissions at the vent site. The deep water after flowing through the K-rich basalts crosses into carbonate formations. This process is highlighted in samples collected from the carbonate aquifer of the Riardo Plain. In connection with the Valdassano fault, CO_2-rich fluxes have been detected in local mineral groundwater wells. The CO_2-rich waters also show the highest content of chemical elements deriving from the alteration of K-rich basalts. These waters show both K-rich (volcanic) and carbonate (bicarbonate–earth

alkaline) features. This process/dynamic is recorded through the variation of the Mg/Ca, Sr/Ca and Ba/Ca ratios, from 0.5 to 0.1, 10 to 2, and 0.25 to 0.05, respectively.

The Suio thermo-mineral springs show completely different chemical characteristics compared to Riardo and eastern mineral waters.

Conversely, the second aquifer (still belonging to the HKS series) is more superficial and is originated within the western side of the caldera and not influenced by carbonate hydrolysis.

(b) Groundwaters flowing through pyroclastic and/or lavas of the last eruptive period show different chemical features compared to aquifer (a): low K and F, no Fe, and As and no correlation between Mg and trace elements (e.g. Li, Mn), while the Na + Cl/Mg ratio ranges between 0.40 and 0.65. Also these waters may (or may not) interact with carbonate rocks and/or waters; however, the process should occur superficially and it is limited on time. Similar to aquifer (a) the Mg/Ca ratio is between 0.5 and 0.1 and the B/Li is constantly close to 5. This latter value is the same for all the Roccamonfina volcanic waters independently from age and aquifer's lithology.

(c) The last type of collected water, found in the area N-NE side of the volcano shows typical bicarbonate–earth alkaline facies. These waters show only features from a carbonate aquifer without interactions with volcanic rocks and waters.

The anthropic/human contamination of Roccamonfina waters is different from area to area: very low within the caldera and with a higher impact on nearby the plains around the volcano. The increase of nitrates and sulfates is the main evidence of such a contamination. This is mainly related to the large use of fertilizers for agricultural practices and the presence of important farm wastes (usually directly discharged into the soil and then leaking into the table water). Similarly, the unusual high content of U has been also associated with the use of U–S–N rich fertilizers.

The Roccamonfina volcanic waters are of high quality for human purposes; however, the bad practices of using too much fertilizers and introducing farm wastes directly in soils (and then in groundwaters) should be seriously taken into account, and it is a clear warning for local authorities to be more careful and to continuously monitor local practices in order to protect the water resource.

References

Allocca V, Celico F, Celico P, De Vita P, Fabbrocino S, Mattia C, Monacelli G, Musilli I, Piscopo V, Scalise AR, Summa G, Tranfaglia G (2007) Carta Idrogeologica dell'Italia Meridionale. Istituto Poligrafico e Zecca dello Stato, Rome

Al-Shawi A, Dahl R (1995) Determination of Thorium and Uranium in nitrophasphate fertilizer solution by ion chromatography. J Chromatogr A 706:175–181

Appleton JD (1972) Petrogenesis of Potassium-rich Lavas from the Roccamonfina Volcano, Roman Region, Italy. J Petrol 13(3):425–456

Ballini A, Frullani A, Mezzetti F (1989) La formazione piroclastica del tufo trachitico Bianco ("white trachitic tuff—WTT auctorum) del vulcano di Roccamonfina. Boll GNV 2:557–574

Buccianti A (1997) Multivariate analysis to investigate Cl distribution in rocks from different settings. Math Geol 29:349–459

Capelli G, Mazza R, Trigari A, Catalani F (1999) le risorse idriche sotterranee strategiche nel distretto vulcanico di Roccamonfina (Campania nord-occidentale). Atti del 3° convegno nazionale sulla protezione e gestione delle acque sotterranee per il III millennio, in Quaderni di Geologia Applicata. Pitagora, Ed, Bologna

Capuano P, Continisio R, Gasparini P (1992) Structural setting of a typical alkali-potassic volcano: Roccamonfina, southern Italy. J Volcanol Geotherm Res 53:355–369

Celico P (1983) Idrogeologia dei massicci carbonatici, delle piane quaternarie e delle aree vulcaniche dell'Italia centro-meridionale (Marche e Lazio meridionali, Abruzzo, Molise e Campania). Quaderni della Cassa del Mezzogiorno 4/2, p 225

Celico P (1988) Prospezioni Idrogeologiche. Liguori Editore, Napoli

Celico P, Civita M, Corniello A (1977) Idrogeologia del margine nord-orientale della conca campana (Massicci dei Tifatini e del Monte Maggiore). Mem e note Ist Geol Appl 13:1–29 Napoli

Celico P, De Gennaro M, Ferreri M, Ghiara MR, Russo D, Stanzione D, Zenone F (1980) Il margine orientale della piana campana: indagini idrogeologiche e idrogeochimiche. Periodico di Mineralogia-Roma 49:241–270

Chiesa S, Floris B, Gillot PY, Prosperi L, Vezzoli L (1995) Il Vulcano di Roccamonfina. In: ENEA (ed) Lazio Meridionale. ENEA, pp 128–150

Chiodini G, Frondini F (2001) Carbon dioxide degassing from the Albani Hills volcanic region, Central Italy. Chem Geol 177:67–83

Cole PD, Guest JE, Uncan AM (1993) The emplacement of intermediate volume ignimbrite: a case study from Roccamonfina volcano, Southern Italy. Bull Volcanol 55:467–480

Corniello A (1988a) Considerazioni idrogeologiche su talune acque minerali e termominerali della provincia di Caserta. Mem Soc Geol Ital 41

Corniello A (1988b) Le acque minerali e termominerali della Provincia di Caserta. Atti 74° Congr Soc Geol Ital Sorrento

Cuoco E (2009) Investigations of natural and anthropogenic processes affecting groundwaters geochemistry of the Caserta Province (Southern Italy). PhD thesis

Davis JC (1986) Statistical and data analyses in geology. Wiley, New York

De Rita D, Giordano G (1996) Volcanological evolution of Roccamonfina volcano (Italy): origin of the summit caldera. In: Mc Guire et al. (eds) Volcano instability on the Earth and other planets. Geol Soc Spec Publ. 110:209–224

Federico C, Aiuppa A, Favara R, Gurrieri S, Valenza M (2004) Geochemical monitoring of groundwaters (1998–2001) at Vesuvius volcano (Italy). J Volcanol Geotherm Res 133:81–104

Gambardella B, Marini L, Maneschi I (2005) Dissolved potassium in the shallow groundwaters circulating in the volcanic rocks of central-southern Italy. Appl Geochem 20:875–897

Giannetti B (1990) Strutture neotettoniche presenti nel tufo trachitico bianco del vulcano di Roccamonfina. Boll Ser Geol Ital 109:195–206

Giannetti B (1996) The geology of the Yellow Trachytic Tuff, Roccamonfina Volcano, Italy. J Volcanol Geotherm Res 71:53–72

Giannetti B (2001) Origin of the calderas and evolution of Roccamonfina volcano (Roman region, Italy). J Volcanol Geotherm Res 106:301–319

Giannetti B, De Casa G (2000) Stratigraphy, chronology, and sedimentology of ignimbrites from the white trachytic tuff, Roccamonfina Volcano, Italy. J Volcanol Geotherm Res 96:243–295

Giannetti B, Luhr JF (1983) The White Trachytic Tuff of Roccamonfina volcano (Roman region, Italy). Contr Min Petr 84:235–252

Giannetti B, Masi U (1989) Trace-element behavior weathering of Leucite in potassic rocks from the Roccamonfina volcano (Campania, southern Italy) and environmental implications. Lithos 22:317–324

Giggenbach WF (1988) Geothermal solute equilibria. Derivation of Na–K–Mg–Ca-geoindicators. Geochim Cosmochim Acta 52:2749–2765

Giordano G, Naso G, Scrocca D, Funiciello R, Catalani F (1995) Processi di estensione e circolazione di fluidi a bassa termalità nella Piana di Riardo (Caserta, Appennino Centro-Meridionale). Boll Soc Geol Ital 114:361–371

Ippolito F, Ortolani F, Russo M (1973) Struttura marginale dell'Appennino Campano: reinterpretazione di dati di antiche ricerche di idrocarburi. Mem Soc Ital 12:227–250

Joreskog KG, Klovan JE, Reyment RA (1976) Geological factor analyses. Elsevier, New York

Lima A, Albanese S, Cicchella D (2005) Geochemical baselines for the radioelements K, U, and Th in the Campania region, Italy: a comparison of stream-sediment geochemistry and gamma-ray surveys. Appl Geochem 20:611–625

Luhr JF, Giannetti B (1987) The Brown Leucitic Tuff of Roccamonfina volcano (Roman region, Italy). Contr Min Petr 95:420–436

Massart DL, Vandeginste BGM, Deming SN, Michotte Y, Kaufman L (1988) Chemometrics: a textbook. Elsevier, Amsterdam

Nicotera P, Civita M (1969) Idrologia della piana del basso Garigliano. In: Mem e note di geologia applicata, vol II. Napoli

Panno SV, Hackley KC, Hwang HH, Kelly WR (2001) Determination of the sources of nitrate contamination in karst springs using isotopic and chemical indicators. Chem Geol 179:113–128

Paone A (2004) Evidence of crustal contamination, sediment, and fluid components in the companion volcanic rocks. J Volcanol Geotherm Res 138:1–26

Pawar NJ, Shaikh IJ (1995) Nitrate pollution of groundwaters from shallow basaltic aquifers, Deccan Trap Hydrologic Province, India. Environ Geol 25:197–204

Peccerillo A (2005) Plio-Quaternary Volcanism in Italy. Springer, Berlin, p 365

Peccerillo A, Manetti P (1985) The potassium alcaline volcanism of central-southern Italy: a review of the data relevant to petrogenesis and geodynamic significance. Trans Geol Soc S Afr 88:379–394

Reyment RA (1997) Multiple group principal component analysis. Math Geol 29:1–16

Rouchon V, Gillot PY, Quidelleur X, Chiesa S, Floris B (2008) Temporal evolution of the Roccamonfina volcanic complex (Pleistocene), Central Italy. J Volcanol Geotherm Res 177:500–514

Steinich B, Escolero O, Marin LE (1998) Salt-water intrusion and nitrate contamination in the Valley of Hermosillo and El Sahuaral coastal aquifers, Sonora. Mex Hydrogeol J 6:518–526

Tesoriero A, Pankow J (1996) Solid solution partioning of Sr^{2+}, Ba^{2+} and Cd^{2+} to calcite. Geochim Cosmochim Acta 60(6):1053–1063

Valentine GA, Giannetti B (1995) Single pyroclastic beds deposited by simultaneous fallout and sorge processes: Roccamonfina volcano, Italy. J Volcanol Geotherm Res 64:129–137

Watts MD (1987) Geothermal exploration of Roccamofina Volcano, Italy. Geothermics vol 16 5/6

Wendlandt RF, Eggler DH (1980) The origin of potassic magmas 1. Melting relations in the system $KAlSiO_4$–Mg_2SiO_4–SiO_2 and $KAlSiO_4$–MgO–SiO_2–CO_2 to 30 kilobars. Am J Sci 280:385–420

Wilbur S, Soffey E (2004) In: McCurdy (ed) Real world analysis of trace metals in drinking water using the Agilent 7500ce ICP-MS with ORS Techonology